Accepted Manuscript

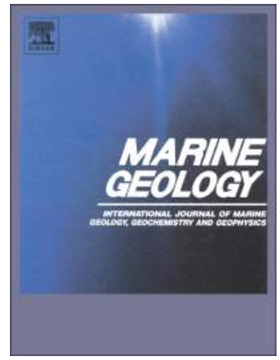

Algal reefs (Coralligenous) from glacial stages: Origin and nature of a submerged tabular relief (Hyblean Plateau, Italy)

Valentina Alice Bracchi, Daniela Basso, Alessandra Savini, Cesare Corselli

PII: S0025-3227(18)30277-9
DOI: https://doi.org/10.1016/j.margeo.2019.02.008
Reference: MARGO 5920

To appear in: *Marine Geology*

Received date: 28 June 2018
Revised date: 18 January 2019
Accepted date: 26 February 2019

Please cite this article as: V.A. Bracchi, D. Basso, A. Savini, et al., Algal reefs (Coralligenous) from glacial stages: Origin and nature of a submerged tabular relief (Hyblean Plateau, Italy), Marine Geology, https://doi.org/10.1016/j.margeo.2019.02.008

Algal reefs (Coralligenous) from glacial stages: origin and nature of a submerged tabular relief (Hyblean Plateau, Italy)

Valentina Alice Bracchi

Milano-Bicocca University, Department of Earth and Environmental Sciences, Piazza della Scienza 4, 20126, Milan, Italy, valentina.bracchi@unimib.it

Daniela Basso

Milano-Bicocca University, Department of Earth and Environmental Sciences, Piazza della Scienza 4, 20126, Milan, Italy, daniela.basso@unimib.it

Alessandra Savini

Milano-Bicocca University, Department of Earth and Environmental Sciences, Piazza della Scienza 4, 20126, Milan, Italy, alessandra.savini@unimib.it

Cesare Corselli

Milano-Bicocca University, Department of Earth and Environmental Sciences, Piazza della Scienza 4, 20126, Milan, Italy, cesare.corselli@unimib.it

Corresponding author:

Valentina Alice Bracchi

University of Milano - Bicocca, Department of Earth and Environmental Sciences, Piazza della Scienza 4, 20126, Milan, Italy, valentina.bracchi@unimib.it

ABSTRACT

In the framework of the Italian multidisciplinary research project "Mud volcanoes Ecosystem study - Sicily Channel", cores MV02_GC01 and MV03_GC02 were recovered from a tabular relief at 140 m water depth, to investigate the nature of such uncommon shallow seep-related morphology trough micro- and macro-paleontological, mineralogical, sedimentological and geochronological analyses. Both cores record muddy surficial sedimentation, hosting a strictly circalittoral molluskan death assemblage typical of mobile substrate, coherent with the present-day seafloor depth and environment. The core bottom recovered a biogenic framework, in which the molluskan fossil assemblage is characteristic of shallow-water, possibly infralittoral, representing a past sea level low stand. The biogenic framework shows structure and composition that are similar to present day algal reefs indicated as coralligenous build-ups. Both cores recorded the Holocene transgression. Core MV02_GC01 is longer and its basal section records cobbles and pebbles of both terrigenous and biogenic origin partially covered by a dark patina, and finely preserved *Halimeda* sp. fragments. The dark patina reveals a fibrous nature, often containing framboid pyrite crystals, ankerite, but no organic matter. We interpret the dark patina level as the last lowstand, possible forming in a lagoon-like paleoenvironment. Below such level, another coralligenous build-up occurs, U/Th dated to MIS 6, in agreement with the available seismic interpretation. The tabular relief lays up to 10 m above the surrounding seafloor and reveals a complex inner architecture, in which at least two generations of coralligenous build-ups shaped its geomorphological development, and the local tectonic activity contributed to its uplift.

KEYWORDS

Mediterranean; Sicily Channel; MIS 6; poliphasic architecture; algal reef; fossil benthic association

1. INTRODUCTION

The Italian multidisciplinary program Mud volcanoes Ecosystem Study - Sicily Channel (MESC) provided a detailed mapping of a shallow mud-volcanoes province located on the outer shelf of the western Malta Plateau (MP) (Fig. 1A-1B) (Max et al., 1993, Holland et al., 2003, Savini et al. 2007, 2009). Different seepage-related seabed morphologies typify the province. Plumes on echosounder profiles (Holland et al., 2006, Savini et al., 2009), collection of direct measures of methane anomalies in seawater (Holland et al., 2006) and geochemical markers (Fe, As, Sb and Mo) of fluid ascending towards the sediment surface (Cangemi et al., 2010), documented gas emission in the province. In addition, an autonomous underwater vehicle (Savini et al., submitted) imaged shallow gas migration pathways recently.

Savini et al. (2009) described at least two shallow seep-related seafloor morphologies: domes and ridges, the latter here referred to as tabular reliefs.

Savini et al. (2009) reported a preliminary description and results of the investigation of cores MV02-GC01 and MV03-GC02 collected from the largest tabular relief. The nannofossil associations from the upper sections of both cores recorded the abundance of typical Holocene species, and in particular *Emiliania huxleyi* (Lohm.) Hay e Mohler, 1967. This suggests a post-Last Glacial Maximum (LGM) age for this section of both cores (Savini et al., 2009). The decrease of *E. huxley*, the occurrence of the cold-water species *Coccolithus pelagicus* (Wallich) J. Schiller, 1930, the abundance of typical Pleistocene species, and the occurrence of reworked species in the basal part of both cores, suggest an older age for such sections (Savini et al., 2009).

Algal concretions have been described in both studied cores (Savini et al., 2009). The occurrence of monumental biogenic frameworks along the present-day Mediterranean shelf is well known in literature (among others Martin et al., 2014). After the LGM regression, present-day living algal reefs indicated as coralligenous build-up (Cb) started forming during the Holocene sea-level rise, in a phase of climate warming (Ballesteros, 2006). In the past, active bioconstruction and accretion of algal reefs are typically associated to warm climate phases (Basso et al., 2007, Bracchi et al., 2014, 2016). Through appropriate and detailed sedimentological, paleontological and geochronological analyses, the aim of this study is to define the nature and architecture of the tabular relief, to clarify its origin, and establish the timing and role of the Cb in its development.

1.1 Study area

The Hyblean plateau (HP) belongs to the Pelagian block, a part of the African foreland in the SE of Sicily (Burrolet et al., 1978, Grasso & Reuther, 1988): it represents a large structural unit including the Sicily channel. The outer shelf of the western Malta Plateau (MP) is the seaward counterpart of the HP on mainland Sicily, limited by the Malta escarpment to the E, by the Ragusa-Scicli and Comiso-Agate faults systems to the W and by the Gela Nappe to the N (Carbone et al., 1984). Meso-Cenozoic succession of carbonate sediments and marls, settling on a crystalline continental basement of unknown age, characterize the MP. The thickness of the Meso-Cenozoic succession is 10 km in the central part, but it reduces to 5-6 km in the northeastern part (Agosh, 1959, Bianchi et al., 1987). In the sedimentary succession, mafic volcanics of different ages occur (Barberi et al., 1974, Patacca et al., 1979, Grasso et al., 1983). Max et al. (1993) have reconstructed the stratigraphy of the western-central part of MP recognizing six seismo-stratigraphic units, from the Messinian low-stand to the recent, representing cycles of sedimentation. Thickness of Plio-Quaternary sediments forming the seismo-stratigraphic units ranges between less than 30 m eastward and more than 100 m westward (Finetti, 1984, Max et al., 1993). Stacked progradational deposits of Quaternary age show reduced thickness, and appear separated by unconformities suggesting low subsidence rates (Gardiner et al., 1993, Max et al., 1993).

The present-day shelf is a low-angle platform dipping gently southwards offshore, towards Malta. A strong decrease in the width of the continental shelf probably occurred during glacial periods. Vai and Cantelli (2004) suggested that the edge of the plateau coincided with the seashore during the LGM. Bioclastic material dominates present-day sediment along the outer shelf, with clay and silt winnowed by currents (Butler et al., 1997).

Different seabed morphologies like cones, domes and tabular relief features have been reported in the area of the MP, correlated with gas emission from shallow marine sediments (Savini et al., 2009). Tabular reliefs (Fig. 1A-F) occur in the outer shelf of the western margin of the area investigated by Savini et al. (2009). All of them show NNW-SSE trending distribution, reflecting patterns of local tectonic. They outcrop in a bathymetric range between 140 and 170 m water depth (wd) and rise almost 10 m above the surrounding seafloor (Fig. 1B-C, Savini et al., 2009). Reliefs are characterized by large, tabular, sub-elongated morphologies (Fig. 1C-D) bearing evidence of the evolution of the coastal facies under the Quaternary sea-level fluctuations (Savini et al., 2009). The largest one reaches 2000 m at its long axis and 500 m at its short axis (Fig. 1C-D). Generally, the reliefs show pronounced sub-vertical flanks and flat tops, which are almost 1 m more depressed than their boundaries. The flat top consists of a matrix of low backscattering, densely spotted by small scale sub-circular cones up to 10 m in diameter and 1 m high with strong acoustic backscattering (Fig. 1D-E) (Savini et al., 2009). Present-day sediments onlap the base of tabular reliefs along their western flanks, whereas marked moats occur on the eastern side (Savini et al., 2009) (Fig. 1F). Evidence of seeps and deposition of authigenic carbonates occur along the flanks of the relief (Savini et al., 2009, Cangemi et al., 2010). Observations by remote operated vehicle at the top clearly showed that authigenic carbonates locally cover the tabular reliefs, fostering the colonization by hard substrate dwellers (*Callogorgia verticillata* (Pallas, 1766)) (Savini et al., 2009, Cangemi et al., 2010).

A very strong and prolonged echo surface reflector, without sub-bottom echoes, marked the sparker record of the MP (U01 unconformity, Savini et al., 2009) (Fig. 1F). U01 unconformity has been identified as the surface of the last low stand; units above U01 include a combination of transgressive and high-stand marine deposits (Max et al., 1993, Savini et al., 2009). Tabular reliefs occur where such unconformity domes up at the seafloor. At first glance, they can be interpreted as erosional remnants that formed, at least partially, during the last sea-level low stand, or before/during the last transgression. Moreover, due to the seismic transparency of their internal structure and the doming up of U01 at their base, the possibility that they are older than the LGM cannot be ruled out (Savini et al., 2009).

2. MATERIAL AND METHODS

Two gravity cores have been collected during the third oceanographic cruise of MESC project, on board the R/V *Universitatis*, in July 2007.

Core MV02_GC01 (36°34.2147'N; 14°30.2232'E), 176 cm long, was sampled on the flank of the tabular relief at 141 m wd (Fig. 1C-D) and divided into two sections: section 1 from cm 0 to cm 76 cm, and section 2 from cm 76 to cm 176 (Fig. 2).

Core MV03_GC02 (36°34.1986'N; 14°29.9800'E), 77 cm long, was sampled at 144 m depth, on the flat top of the tabular relief (Fig. 1C-1D; Fig. 2) .

Opening, description and sub-sampling have been conducted at the geobiological laboratories of the University of Milano-Bicocca, Department of Earth and Environmental Sciences (DISAT), Italy. Qualitative and quantitative study of molluskan death assemblages and algal concretions have been performed.

Each core has been sub-sampled at any evident change in texture or color. Sixteen samples (M0-M15) have been obtained from core MV02_GC01, and 11 samples (M0-M10) from core MV03_GC02 (Fig. 2).

Each sample has been wet sieved for grain size analyses and for the extraction of the biogenic components. The manual picking of >1mm residue was conducted for the analysis of the molluskan death assemblage. Mollusks were identified, described, and counted following the methods of Basso & Corselli (2007). The ecological interpretation of the death assemblage has been conducted based on the model of Pérès and Picard (1964) and Bellan-Santini et al. (1994). French definition of biocoenoses and acronyms are here indicated following Pérès and Picard (1982) and Basso and Corselli (2002).

Twenty-five thin sections of biogenic framework, collected from the base of both cores, have been prepared for non-geniculate red algae identification performed using a polarizing microscope. The taxonomy of non-geniculate red algae follows the biological systematics framed by Woelkerling (1988), as revised by several subsequent contributions (early summary in Bressan and Babbini, 2003; Pezzolesi et al., *in press*), and adapted to paleontology (Braga et al., 1993, Basso, 1994, 1995, Basso et al., 1996, 1997, 2007, Di Geronimo, 2007, Hrabovský et al., 2015).

Chemical and mineralogical analyses have been conducted on picked fragments of well-preserved biogenic and terrigenous particles coated with a black patina, occurring in the section 132-156 cm of core MV02_GC01. In particular, 12 fragments have been mounted on stubs with silver glue for Scanning Electron Microscopy (SEM) observations and Energy Dispersive X-Ray (EDX) Spectroscopy measures. The intensity current of measurement was 190 picoA at 20 kV; the beam range was 225 nm at a working distance of 24 mm. To investigate the nature of the dark patina on mollusk shells and lithoclasts, X-Ray diffraction analyses have been conducted at DISAT, whereas Total Organic Carbon (TOC) and Rock-Eval (RE) pyrolysis analysis were performed in the Oil & Gas Laboratory of ENI - San Donato Milanese, together with observations of polished thin sections. Finally, six fragments from the biogenic framework of core MV02_GC01 (Fig. 2) have been selected to conduct U/Th disequilibrium dating by using a multicollector induction-coupled plasma mass spectrometry at the University of Bern, Switzerland.

3. RESULTS

3.1 MV02_GC01

3.1.1 LITHOLOGICAL DESCRIPTION

Section 1 presented a transition from pure mud (5Y 5/3 olive gray) at the top, to gravelly sand to the bottom (Fig. 2). Section 2 was characterized by 5Y 4/2 olive gray coarse sediment at the top (cm 76), turning to angular fragments with matching edges, as they formed originally a single block of biogenic framework, probably fragmented by coring (Fig. 2, Fig. 3A). The biogenic framework was mainly composed of encrusting coralline algae accompanied by bryozoans (Fig. 3A). Olive muddy sediment filled the cavities among blocks (Fig. 2, Fig. 3A).

Between 132 and 156 cm, a layer occurred (Fig. 2, Fig. 4), from which sample M12 was collected. This level is dark colored (from 5Y3/2 dark olive gray to 2.5Y 4/0 dark gray and 2.5Y 3/0 very dark gray) and composed of sandy gravel with pebbles and cobbles up to 7 cm (Fig. 4), and about 80% of gravel-sized components. Among them, at least three typologies of grains have been identified (Fig. 4, Fig. 5). Group 1 (Fig. 4B) contains rounded, smooth, terrigenous pebbles, derived from the

Ragusa Formation (Carbone et al., 1984), white or gray, with spots of black patina. Group 2 (Fig. 4C) contains biogenic gravel-sized fragments and pebbles mostly represented by mollusk shells and fragments, or algal concretions with sandy-muddy matrix filling the cavities. Group 3 (Fig. 4D, Fig. 5) contains biogenic pebbles and cobbles almost totally covered by black patina, including both shell fragments (Fig. 5A-F) and cobble-size elements, composed of several particles glued together by the black smooth patina (Fig. 5G-5H). Group 2 and 3 cobbles and pebbles are more abundant than those of Group 1.

3.1.2 MOLLUSKAN FOSSIL ASSEMBLAGES

A total of 2598 specimens have been picked up, belonging to 207 mollusk species (Appendix 1). Species representative of the circalittoral zone occurred in the whole section 1 (samples from M0 to M7). They include exclusive and preferential species of the circalittoral and bathyal zones, belonging to the biocoenoses of the coastal detritic (DC), the coastal terrigenous mud (VTC), the deep mud (VP), together with other deep-water species (Fig. 6A, Appendix 1, Table 1).

On the contrary, abundant circalittoral hard-substrate species (C) and infralittoral species (HP and AP biocoenoses) occurred in samples M8 to M11 (Fig. 6A, Appendix 1, Table 1).

Sample M12 collected in the dark level between 132 and 156 cm (Fig. 2, 4 A-D), was very distinctive. It delivered 490 specimens belonging to 59 mollusk species pointing to a strictly infralittoral assemblage. A total of 13 species (65%) belonged to infralittoral biocoenoses, like HP and AP (Fig. 6A, Table 1). Meso-infralittoral species were also identified (Table 1). Only 30% of the identified species were related to C and DC biocoenoses (Fig. 6A, Table 1). It is remarkable that in sample M12 many mollusk shells were abraded and/or broken and consequently not recognizable, and their level of conservation very low. On the other hand, several specimens of mollusks (Fig. 5D), even if recognizable, were almost completely covered by the black patina. Moreover, no relationship existed between the occurrence of the black patina and the state of conservation of the mollusk shells.

Below M12, circalittoral species quantitatively dominated the molluskan assemblage of samples M13, M14 and M15, although no exclusive species has been recognized. The M13 molluskan assemblage recorded two species preferential of DC and one of C biocoenosis (Fig. 6A, Table 1)

3.1.3 CALCAREOUS ALGAE

A biogenic framework, formed mostly by encrusting coralline algae, characterized the samples from M8 to M15 (except for sample M12) (Fig. 2, Fig. 3A). The bioconstruction was massive and composed of: *Lithophyllum stictiforme* (Areshoug) Hauck (1877), *Titanoderma pustulatum* (J.V.Lamouroux) Nägeli in Nägeli & Cramer 1858, *Titanoderma* sp., *Phymatoliton calcareum* (Pallas) Adey & Mc Kibbin (1970), *Neogoniolithon* sp. and *Mesophyllum* sp. The first two species occurred in all samples, while the other taxa were less common.

In contrast, in sample M12 coralline algae were present as fragments, millimeter to centimeter-sized, sparse within the above-described coated elements (Fig. 7H). Identified species were *Titanoderma* sp. (Fig. 7A-B), *L. stictiformae* (Fig. 7C-D) and *Mesophyllum* sp. The abundance of well-preserved fragments of the green calcareous alga *Halimeda* sp. is remarkable (Fig. 7B-D-E). On thin section, the skeletal features of calcareous red and green algae was well detectable, although a number of them may showed some dark-colored surfaces (Fig. 7E-H).

3.2 MV03_GC02

3.2.1 LITHOLOGICAL DESCRIPTION

Three different lithologies have been recognized along the core (Fig. 2). Gravel (2.5YR 5/6 olive), mostly of biogenic nature, characterized the first 10 cm. Mud (5Y 5/2 olive gray) with sparse white (2.5Y 7/6) and yellow (2.5Y 8/2) clasts characterized the central interval, from 10 to 35 cm. Angular fragments with matching edges were recovered from 35 to 81 cm of core, originally forming a single block of biogenic framework probably fragmented by coring (Fig. 2, Fig. 3B-C). Encrusting coralline algae (yellow and white), accompanied by bryozoans mostly formed the framework, within coarse biogenic sediment and mud (5Y 6/3 pale olive).

3.2.2. MOLLUSKAN ASSEMBLAGES

A total of 1388 specimens belonging to 126 species have been collected (Appendix 2).

A circalittoral death assemblage characterized the first 10 cm of the core, with the occurrence of species belonging to both hard substrate (C) and coarse soft substrate (DC) biocoenoses (Fig. 6B, Table 2). In the muddy interval (10 - 35 cm), species belonging to VP, C, and DC biocoenoses have been identified (Fig. 6B, Table 2). The hard bottom sampled from 35 cm down to the basis of the core, showed a mixing of species. We identified an infralittoral molluskan assemblage, with species linked to the HP and AP biocoenoses or widely distributed infralittoral species (Fig. 6B, Appendix 2, Table 2). They occurred together with C and DC species (Fig. 6B, Table 2), although quantitatively less important.

3.2.3 CALCAREOUS ALGAE

Calcareous encrusting coralline red algae belonging to the species *L. stictiforme*, *T. pustulatum* and *Phymatolithon* sp. characterized the biogenic framework. The framework was dense, although mud was abundant inside the cavities.

3.3 SEM OBSERVATION, MINERALOGICAL AND GEOCHEMICAL ANALYSES

EDX analyses on fragments with black coating (Fig. 8A-B) revealed the occurrence of Ca-sulfate and Al-Mg silicate (Fig. 8A), and high C peak (Fig. 8B). EDX on encrusting coralline algae (Fig. 8D), although covered by black patina, recorded the occurrence of a high-Mg calcite peak (Fig. 8C). Under SEM the surface of the black patina showed a fibrous and very porous nature, with common iron-sulphur framboid spherules (Fig. 8E), observed also on polished thin sections (Fig. 8F).

A shell, partially encrusted by the black patina (Fig. 4D, Fig. 9A-B), revealed, once cut, a thin encrustation by coralline algae (Fig. 9D, black arrow). The X-Ray diffraction of the dark coralline encrustation showed 51% of high-Mg calcite and 38% of calcite, which is fully compatible with the mineralogy of coralline algae (Basso, 2012) (Fig. 9D).

X-ray diffraction analysis on dark lithoclasts (Fig. 4B, Fig. 9C) showed a composition of quartz (91%), calcite (8%) and 1% of ankerite (Fig. 9E).

TOC and RE pyrolysis analysis excluded the occurrence of any type of organic matter.

3.4 U/Th DATING

Samples B5 and B6 have been considered suitable for U/Th dating, and provided an age of 144±6 ky BP, thus dating the basal section of core MV02_GC01 to Marine Isotope Stage (MIS) 6 (Fig. 2). On the contrary, samples B1, B2, B3 and B4 resulted to be unsuitable for U/Th dating, because the initial $^{234}U/^{238}U$ ratio was not reliable.

4. DISCUSSION

Both cores showed a remarkable variation of sediment texture, fossil assemblages, and related paleoenvironmental reconstructions.

4.1 PALEOENVIRONMENTAL RECONSTRUCTION

A circalittoral fossil assemblage of soft bottom species is present in the upper portion of both cores, which corresponds to present-day wd (Fig. 2, Fig. 6). Similar features are observed in the modern hemipelagic sediments of the Strait of Sicily (Tonarelli et al., 1993, Cangemi et al., 2010, Tranchida et al., 2010, Micallef et al., 2011). From the present-day circalittoral conditions featured at the top, the downcore records grade toward shallow water, infralittoral paleoenvironments (Fig. 2, Fig. 6). Shallow water conditions are reconstructed for those core sections composed of sandy gravel and biogenic framework (Fig. 2, Fig. 6). The related molluskan assemblage is a complex mixing of species linked to AP and HP biocoenoses, together with the contribution of C, DC and hard-substrate species, issued by the biogenic framework (Fig. 6, Table 1, Table 2).

The main features of the biogenic framework are similar to present-day Mediterranean algal reefs indicated as Cb, spanning the depth 4-140 m (Sarà, 1966, Ballesteros, 2006). Although the Cb is defined as a circalittoral biocoenosis (Pérès and Picard, 1964), it is reported also for shallow-water, infralittoral, environments (e.g. Sarà, 1969, Laborel, 1987, Argenti et al., 1989), also from Pleistocene examples (Bracchi et al., 2014, 2016). Consequently, considering the main features of the studied biogenic framework and associated death assemblage, we can interpret it as a fossil example of shallow-water Cb.

The development of build-ups has obvious geomorphological implications, by forming solid substrates with topographic reliefs that shape the seafloor (Ballesteros, 2006, Bracchi et al., 2017). The occurrence of this kind of biogenic frameworks within the architecture of the tabular relief suggests a role in its vertical development. The recovery of biogenic framework does not cover the whole cores. However, we consider that exactly the occurrence of this rigid framework, as indicated also by the seismic record (Savini et al., 2009), prevented the gravity corer from penetrating deeper. Consequently, we suggest that the biogenic framework likely continues further below, into the relief. Moreover, the homogeneity of the seismic signal (Fig. 1F), as already reported by Savini et al. (2009), supports the idea that Cb can be also laterally continuous within the tabular relief.

The successions recorded above M12 and the entire core MV03_GC02 are consistent with the Holocene shoreline backstepping following a general deepening upward (Fig. 2, Fig. 10). Above M12, we can argue that Cb developed during the Holocene sea level rise, in a bathymetric interval compatible with its growth, surely in a transgressive phase corresponding to a climate colder than the present (Fig. 10). The Cb of core MV02-GC01 above sample M12 has a thickness of 55 cm. Basing upon literature reports on growth rate, ranging between 0.2 and 2 mm/yr (Sartoretto et al., 1996, Di Geronimo et al., 2002), this Cb needed from 275 to 2750 years to develop during Holocene marine transgression, until the final drowning by sediments.

4.2 SAMPLE M12 OF CORE MV02-GC01

Cb is missing in the interval 132-156 cm corresponding to sample M12 of core MV02_GC01 (Fig. 2, Fig. 4 A-D), and this is probably due to the extreme shallow wd reached in correspondence of such layer, coupled with episodic terrigenous input testified by the occurrence of rounded, smoothed, quartz terrigenous pebbles transported from inland. This core section is representative of a past sea level low stand. The molluskan fossil assemblage is compatible with strictly shallow water condition (few meters wd) (Fig. 5, Table 1). On the other hand, the report of rounded terrigenous clasts and shell remains is consistent with the occurrence of high hydrodynamics in shallow water by currents or wave actions. Transport also explains the complex mixing of mollusks in the fossil assemblage. The occurrence of *Halimeda* sp. fragments supported a shallow paleo-depth reconstruction. *Halimeda* sp. is a genus of green macroalgae, with a thallus formed by flattened, calcified segments of various shapes, connected by non-calcareous joints. Mediterranean *Halimeda* is comparably less calcified (aragonite) than its tropical relatives (Granier, 2012). The species *Halimeda tuna* (J. Ellis & Solander) J.V. Lamouroux 1816 is reported as very common in the depth range of 30-50 m wd in the Mediterranean, where it characterizes the shallow Cb settings, in pits and dim light conditions (Pérès and Picard, 1964, Ballesteros, 2006). Dim light in shallow settings may occur under overhanging structures or in turbid water (Coletti et al., 2018), which is expected at the studied site because of the observed terrigenous sedimentation. The observed occurrence of *Halimeda* sp. segments and their conservation requires a deposition *in situ* and a fast burial. Therefore, we suggest that *Halimeda* sp. developed in shallow water under dim light conditions, and that post-mortem loose segments of such species have been rapidly buried into sediments.

In the same layer, a very distinctive aspect is the occurrence of a black patina. Mineralogical analyses revealed that it is a fibrous porous material, with FeS framboid spherules. Analogous material is reported for cold seeps of Monterey Bay (Stakes et al., 1999), for mud volcanoes and pockmarks on the Nile deep-sea fan (Gontharet et al., 2007), for authigenic carbonates in a pockmark field of the west Alboran basin (Blinova et al., 2011) and for the Bonaccia carbonates in the Adriatic Sea (Capozzi et al., 2012). Our surveyed area is presently affected by gas seepage phenomena and production of authigenic carbonates, in the form of thick crusts on domes and tabular relief (Max et al., 1993, Holland et al., 2003, 2006, Savini et al. 2007, 2009, Cangemi et al., 2010), whereas present-day mud volcanism is not evident (Savini et al., 2009). Moreover, the tabular reliefs are few kilometers from the Vega Oil field (active oil extraction), and elongated in NNW-SSE direction that is the main path for seeps provided by NW-SE tectonic lineaments (Savini et al., submitted). Past phenomenon of fluid emission cannot be ruled out, even if the nature of this patina remains problematic, because, contrarily to our expectations, no trace of organic matter was detected. Some coralline algal fragments show a partial re-crystallization of the skeleton by a yellowish- brownish mineral. Krajewski (2002) reports the replacement of biogenic calcite by catagenic ankerite in the area of Marhøgda bed (Spitsbergen). Ankerite is a Mn/Fe-enriched dolomite occurring as authigenic, diagenetic mineral and as a product of hydrothermal precipitation. Ankerite was detected in our EDX graph (Fig. 9E), and features similar to those observed by Krajewski (2002) were reported in our thin sections (Fig. 7G).

Considering the sea level reconstruction proposed by Lambeck et al. (2004, 2011), the LGM reached 125/130 m below present-day sea level (bls) in the studied area. It has been suggested (Vai and Cantelli, 2004) that the edge of the plateau corresponded to the paleo-seashore during the LGM. Walbroeck et al. (2002) reported the calculated sea level variation for the pre-LGM MIS. The sea level drop during MIS 4 was less important than the LGM one, reaching 100 m bsl, whereas during MIS 6 it reached 160 m bsl. At the same time, we must consider that alternating uplift and subsidence characterized the Neogene and Quaternary in Sicily, and in particular, the Hyblean Plateau underwent periods of volcanism-related uplift during the Pliocene and Pleistocene (Yelling-Dror et al., 1997, Di Martire et al., 2015). The tabular relief, consequently, has been interested by both uplift and important marine regression, testified by the very shallow facies recorded in level M12 of core MV02_GC01, possibly corresponding to the last low stand (MIS 2) (Fig. 2, Fig. 6, Fig. 10). Max et al. (1993) already suggested the development of a deltaic/coastal environment for the last low-stand. We can hypothesize that local variation in water oxygenation and possible restricted circulation in such shallow environments created the conditions for the diagenetic formation of the black patinas.

4.3 DATING AND ORIGIN OF THE RELIEF

U/Th disequilibrium defines the age of the basal portion of core GC02-MV01. The initial $^{234}U/^{238}U$ ratio is the most sensitive indicator of possible mobilization of uranium during diagenesis, with highest values giving older dates (Stirling et al., 1995). In order to achieve a reliable dating, the measurable initial $^{234}U/^{238}U$ ratio should be in equilibrium with the seawater value that corresponds to 1.14±0.03 (Henderson and Anderson, 2003). However, significant variation of this ratio (1.02 to 1.20) have been reported for the Pacific Ocean, although the cause is unclear (Miyake et al., 1966). In the same region, an increase of uranium concentration with wd was also reported (Miyake and Sugimura, 1964). Similarly, Cangemi et al. (2010) report highest value of U concentration for sediments collected in the Sicilian area here investigated. Ratio values measured for our samples range from 1.11 (sample B6) to 1.19 (sample B3). Therefore, at least two of them (samples B5 and B6) have been considered reliable, while sample weathering and diagenesis probably affected the other four samples, and dating is consequently unreliable. Reliable samples are dated 144±6 ky BP, ascribing the basal section of core MV02_GC01 to MIS 6. This age, predating LGM, is in agreement with the observation that the tabular relief occurs where U01 unconformity domes up at the seafloor (Savini et al., 2009).

Local tectonic activity, as already identified by Savini et al. (2009), contributes to the present elevation of the tabular reliefs, up to 10 m above surrounding seafloor. On the other hand, we can argue that at least two generations of biogenic framework (coralligenous), with the interposition of the layer from where sample M12 was collected, superposed and contribute to the vertical growth and geomorphological development of the tabular relief. Based on literature, bioconstruction developed during the transgression phase of warm climate stages in marine terraces cropping out on land (Basso et al., 2007, Bracchi et al., 2014, 2016). In our case, we have evidence of a polyphasic bioconstruction, first accreting during the cold-climate MIS 6 and then accreting in the first phase of the Holocene sea level rise, until the final drowning by mud in the circalittoral zone (Fig. 2). The studied tabular relief outcropped in an area characterized by the lowest thickness of Plio-Quaternary sediments (Finetti, 1984, Max et al., 1993). Condensation and erosion are expected phenomena, probably fostered by the elevation of the tabular relief. These aspects must be considered for explaining the incomplete stratigraphic record. In the case of the studied tabular relief, local tectonic coupling with poliphasic development of biogenic framework created a positive seabed structure with metrical elevation. Present-day deep-water Cb reliefs occurring throughout the Mediterranean could have similarly a polyphasic origin, and this hypothesis would deserve further investigation.

5. CONCLUSION

The multidisciplinary study of the two cores reveals the complex nature of uncommon, shallow seep-related tabular relief, sampled at 140 m wd on the Hyblean Plateau, Sicily Channel.

Both cores record the Holocene sea level rise, with the occurrence of algal reefs indicated as Cb at the base, passing upward to circalittoral fossiliferous sediments. Moreover, core MV02_GC01 collected a peculiar very coarse level corresponding to the last low stand (MIS 2) (pebbles, and cobbles with black patina, strictly infralittoral fossil assemblage, terrigenous contribute). It possibly formed in a lagoon-like paleoenvironment and an older Cb. Basing upon U/Th dating, this older Cb is dated from MIS 6, in agreement with the seismic analysis by Savini et al. (2009). We conclude that Cb contributed to the morphological development and accretion of the tabular relief, which lays up to 10 m above surrounding seafloor, coupling with local tectonic uplift. Major framework builders are the coralline algae (*L. stictiforme*, *T. pustulatum*) and at least two generations of biogenic framework contributed to the tabular relief, with a polyphasic pattern. Finally, we suggest that in both cases the Cb grew during cold climate stages.

6. ACKNOWLEDGEMENTS

VAB is funded through a post-doctoral fellowship in Earth Sciences by the University of Milano-Bicocca. We acknowledge the ship-time through the 2006-2007 Italian PRIN ‘MESC’ program, funded by the Italian Ministry of Research and Technology (MIUR). Dr. Angelo Riva (ENI Geochemistry GEOLAB) is acknowledged for the analyses and fruitful discussions on geochemical results. This is a scientific contribution of Project MIUR - Dipartimenti di Eccellenza 2018-2022.

7. REFERENCES

Agosc, W.B., 1959. Profondità e struttura dell’orizzonte igneo tra Catania e Tunisi dedotte da un profilo aeromagnetico. Bollettino del Servizio Geologico Italiano 80, 51-61.

Argenti, L., Taramelli, E., Matteucci, B., Argano, R., 1989. Notizie preliminari sui popolamenti vagili di formazioni coralligene infralitorali al largo di S. Severa (Roma). Oebalia 15 (1), 287-288.

Ballesteros, E., 2006. Mediterranean coralligenous assemblages: a synthesis of present knowledge. Oceanography and Marine Biology: Annual Review 44, 123-195.

Barberi, F., Civetta, L., Gasparini, P., Innocenti, F., Scandone, R., Villari, L., 1974. Evolution of a section of the Africa–Europe plate boundary; paleomagnetic and volcanological evidence from Sicily. Earth Planetary Science Letters 22 (2), 123-132.

Basso, D., 1994. Study of living calcareous algae by a paleontological approach: the non-geniculate Corallinaceae (Rhodophyta) of the soft bottom of Tyrrhenian Sea (western Mediterranean). The genera *Phymatolithon* Foslie and *Mesophyllum* Lemoine. Rivista Italiana di Paleontologia e Stratigrafia 110(4), 575-596.

Basso, D., 1995. Living calcareous algae by a paleontological approach: the genus *Lithothamnion* Heydrich nom. cons. from the soft bottoms of the Tyrrhenian Sea (western Mediterranean). Rivista Italiana di Paleontologia e Stratigrafia 101, 349-366.

Basso, D., 2012. Carbonate production by calcareous red algae and global change, in: Basso, D., Granier, B. (Eds), Calcareous algae and global change: from identification to quantification. Geodiversitas 34 (1), 13-33.

Basso, D., Corselli, C., 2002. Community versus biocoenosis in multivariate analysis of benthic molluscan thanatocoenosis. Rivista Italiana di Paleontologia e Stratigrafia 108, 153-172.

Basso, D., Corselli, C., 2007. Molluscan paleoecology in the reconstruction of coastal changes, in: Yanko-Hombach, V., Gilbert, A.S., Panin, N., Dolu- khanov, P.M. (Eds.), The Black Sea flood question: changes in coastline, climate, and human settlement, NATO Science Series IV, Earth and environmental Science, Kluwer Academic Press, Dordrecht, pp. 23-46.

Basso, D., Fravega, P., Vannucci, G., 1996. Fossil and living corallinaceans related to the Mediterranean endemic species *Lithophyllum racemus* (Lamarck) Foslie. Facies 35 (1), 275.

Basso, D., Fravega, P., Vannucci, G., 1997. The taxonomy of *Lithothamnium ramosissimum* (Gümbel nonReuss) Conti and *Lithothamnium operculatum* (Conti) Conti (Rhodophyta, Corallinaceae). Facies 37 (1), 167-181.

Basso, D., Nalin, R., Massari, F., 2007. Genesis and composition of the Pleistocene *Coralligène de plateau* of the Cutro Terrace (Calabria, southern Italy). Neues Jahrbuch für Geologie und Paläontologie 244/2, 73-182.

Bellan–Santini, D., Lacaze, J.C., Poizat, C., 1994. Les biocénoses marines et littorales de Méditerranée, synthèse, menaces et perspectives, Collection Patrimoines Naturels, Secrétariat de la Faune et de la Flore/M.N.H.N. 19.

Bianchi, F., Carbone, S., Grasso, M., Invernizzi, G., Lentini, F., Longaretti, G., Merlini, S., Mostardini, F., 1987. Sicilia orientale: profilo geologico Nebrodi-Iblei. Memorie della Società Geololica Italiana 38, 429-458.

Blinova, V.N., Comas, M.C., Ivanov, M.K., Poludetkina, E.N., Matveeva, T.V., 2011. Active mud volcanism in the West Alboran Basin: Geochemical evidence of hydrocarbon seepage. Marine and Petroleum Geology 28, 1483-1504.

Bracchi, V.A., Nalin, R., Basso, D., 2014. Paleoecology and dynamics of coralline-dominated facies during a Pleistocene transgressive–regressive cycle (Capo Colonna marine terrace, Southern Italy). Palaeogeography Palaeoclimatolology Palaeoecology 414, 296-309.

Bracchi, V.A., Nalin, R., Basso, D., 2016. Morpho-structural heterogeneity of shallow-water coralligenous in a Pleistocene marine Terrace (Le Castella, Italy). Palaeogeography Palaeoclimatolology Palaeoecology 454, 101-112.

Bracchi, V.A., Basso, D., Marchese, F., Corselli, C., Savini, A, 2017. Coralligenous morphotypes on subhorizontal substrate: A new categorization. Continental Shelf Research 144, 10-20.

Braga, J.C., Bosence, D.W.J., Steneck, R.S., 1993. New anatomical character in fossil coralline algae and their taxonomic implications. Palaeontology 36, 535-547.

Bressan, G., Babbini, L., 2003. Corallinales del Mar Mediterraneo: Guida alla determinazione, Biologia Marina Mediterranea.

Burrollet, P.F., Mugniot, J.M., Sweeney, P., 1978. The geology of the Pelagian Block: the margins and basins of Southern Tunisia and Tripolitania, in: Nairn, A.E.M, Kanes, W.H., Stehli, F.G. (Eds.), The ocean basins and margins, Plenum Press, NY, pp. 331-359.

Butler, R.W.H., Grasso, M., Gardiner, W., Sedgeley, D., 1997. Depositional patterns and their tectonic controls within the Plio-Quaternary carbonate sand and muds of onshore and offshore SE Sicily (Italy). Marine and Petroleum Geology 14 (7/8), 879-892.

Cangemi, M., Di Leonardo, R., Bellanca, A., Cundy, A., Neri, R., Angelone, M., 2010. Geochemistry and mineralogy of sediments and authigenic carbonates from the Malta Plateau, Strait of Sicily (Central Mediterranean): Relationships with mud/fluid release from a mud volcano system. Chemical Geology 276, 294-308.

Capozzi, R., Guido, F.L., Oppo, D., Gabbianelli, G., 2012. Methane-Derived Authigenic Carbonates (MDAC) in northern-central Adriatic Sea: Relationships between reservoir and methane seepages. Marine Geology 332-334, 174-188.

Carbone, S., Grasso, M., Lentini, F., 1984. Carta Geologica della Sicilia Sud-Orientale, Scala 1:100.000. S.EL.CA., Firenze.

Coletti, G., Basso, D., Corselli, C., 2018. Coralline algae as depth indicators in the Sommières Basin (early Miocene, Southern France). Geobios, 51, 15-30.

Di Geronimo, R., 2007. An account of Pleistocene species of *Lithophyllum* (Corallinaceae, Rhodophyta) from Sicily (Southern Italy). Neues Jahrbuch für Geologie und Paläontologie 244/2, 183-196.

Di Geronimo, I., Di Geronimo, R., Rosso, A., Sanfilippo, R., 2002. Structural and taphonomic analysis of a columnar build-up from Sicily shelf. Géobios 35: 86-95.

Di Martire, D., Ascione, A., Calcaterra, D., Pappalardo, G., Mazzoli, S. 2015. Quaternary deformation in SE Sicily: Insights into the life and cycles of forebulge fault systems. Lithosphere 7 (5), 519-534.

Finetti, I., 1984. Geophysical study of the Sicily Channel rift zone. Bollettino Geofisica Teorica Applicata 24, 3-28.

Gardiner, W., Grasso, M., Sedgeley, D., 1993. Plio-Pleistocene stratigraphy and fault movement of the Malta platform, in: Max, M.D., Colantoni, P. (Eds.), UNESCO Technical Reports in Marine Science, pp. 111–116.

Gontharet, S., Pierre, C., Blanc-Valleron, M.M., Rouchy, J.M., Fouquet, Y., Bayon, G., Foucher, P., Woodside, J., Mascle, J., the Nautinil Scientific Party, 2007. Nature and origin of diagenetic carbonate crusts and concretions from mud volcanoes and pockmarck of the Nile deep-sea fan (eastern Mediterranean Sea). Deep-Sea research II 54, 1292-1311.

Granier, B., 2012. The contribution of calcareous green algae to the production of limestones: a review. Geodiversitas 34 (1), 35-60.

Grasso, M., Lentini, F., Nairn, A.E.M., Vigliotti, L., 1983. A geological and paleomagnetic study of the Hyblean volcanic rocks, Sicily. Tectonophysics 98, 271-295.

Grasso, M., Reuther, C.D., 1988. The western margin of the Hyblean Plateau: a neotectonic transform system on the SE Sicilian foreland. Annales Tectonicæ, vol. II, 2: 107-120.

Henderson, G.M., Anderson, R.F. 2003. The U-series Toolbox for Paleoceanography. Reviews in Mineralogy and Geochemistry 52, 493-531.

Holland, C.W., Etiope, G., Milkov, A.V., Michelozzi, E., Favali, P., 2003. Mud volcanoes discovered offshore Sicily. Marine Geology 199, 1-6.

Holland, C.W., Weber, T.C., Etiope, G., 2006. Acoustic scattering from mud volcanoes and carbonate mounds. Journal of Acoustic Society of America 120 (6), 3553-3565.

Hrabovský, J., Basso, D., Doláková, N. 2015. Diagnostic characters in fossil coralline algae (Corallinophycidae: Rhodophyta) from the Miocene of southern Moravia (Carpathian Foredeep, Czech Republic). Journal of Systematic Paleontology 14, 499-525.

Krajewski, K.P., 2002. Catagenic ankerite replacing biogenic calcite in the Marhøgda Bed (Jurassic), Sassenfjorden, Spitsbergen. Polish Polar Resesarch 23(1), 85-99.

Laborel, J., 1987. Marine biogenic constructions in the Mediterranean: a review. Scientific Rapports Port Cros National Park 13, 97-126.

Lambeck, K., Antonioli, F., Purcell, A., Silenzi S., 2004. Sea level change along the Italian coast during the last 10000 years. Quaternary Science Review 23, 1567-1598.

Lambeck, K., Antonioli, F., Anzidei, M., Ferranti, L., Leoni, G., Scicchitano, G., Silenzi, S., 2011. Sea level change along the Italian coast during the Holocene and projections for the future. Quaternary International 232(1–2), 250-257.

Max, M.D., Kristensen, A., Michelozzi, E., 1993. Small scale Plio-Quaternary sequence stratigraphy and shallow geology of the west-central Malta Plateau, in: Max, M.D., Colantoni, P. (Eds.), UNESCO Technical Reports in Marine Science, pp. 117–122.

Martin, C.S., Giannoulaki, M., De leo, F., Scardi, M., Salomidi, M., et al., 2014. Coralligenous and maërl habitats: predictive modelling to identify their spatial distributions across the Mediterranean Sea, Scientific Reports 4, Article number: 5073.

Micallef, A., Berndt, C., Debono, G., 2011. Fluid flow system of the Malta Plateau, Central Mediterranean Sea., Marine Geology 284, 74-85.

Miyake,Y., Sugimura, Y., 1964. Uranium and radium in the western North Pacific waters, in: Yoshida, K. (Ed.), Studies on oceanography, University of Tokyo Press, pp. 274-278.

Miyake,Y., Sugimura, Y., Uchida, T., 1966. Ratio $^{234}U/^{238}U$ and the uranium concentration in seawater in the western North Pacific. Journal of Geophysical Research 71, 3083-3087.

Patacca, E., Scandone, P., Giunta, G., Liguori, V.,1979. Mesozoic paleotectonic evolution of the Ragusa zone (Southeastern Sicily). Geologia Romana 18, 331-369.

Pérès, J.M., Picard, J., 1964. Nouveau Manuel de Bionomie Benthique de la Mer Méditerranée, Station Marine d'Endoume.

Pérès, J.M., Picard, J., 1982. Major benthic assemblages, in: O. Kinne (Ed.) Marine Ecology V. 5, Part 1, John Wiley and Sons Ltd, Chirchester, pp-373-522

Pezzolesi L., Peña V., Le Gall L., Gabrielson P.W., Kaleb S. et al., in press. Mediterranean *Lithophyllum stictiforme* (Corallinales, Rhodophyta) is a genetically diverse species complex: implications for species circumscription, biogeography and conservation of coralligenous habitats. Journal of Phycology.

Sarà, M., 1966. Un coralligeno di piattaforma (coralligene de plateau) lungo il litorale pugliese. Archivi Oceanografia Limnologia 15, 139-150.

Sarà, M., 1969. Research on coralligenous formations: problems and perspectives. Pubblicazioni della Stazione Zoologica di Napoli 37 (Suppl.), 124-134.

Sartoretto, S., 1994. Structure et dynamique d'un nouveau type de bioconstruction à *Mesophyllum lichenoides* (Ellis) Lemoine (Corallinales, Rhodophyta). Comptes Rendus de l'Académie des Sciences III 317, 156-160.

Sartoretto, S., Verlaque, M., Laborel J., 1996. Age of settlement and accumulation rate of submarine “coralligène” (-10 to -60 m) of the northwestern Mediterranean Sea, relation to Holocene rise in sea level. Marine Geology 130, 317-331.

Savini, A., Corselli, C., Tessarolo, C., Daffonchio, D., Bellanca, A., Danovaro, R., Etiope, G., 2007. Seafloor mapping and acoustic geophysical data of a shallow likely mud-volcanoes province Offshore Sicily (eastern Sicily Channel – Hyblean–Malta plateau). 38 CIESM Congress, 09–13 April 2007, Istanbul.

Savini, A., Malinverno, E., Etiope, G., Tessarolo, C., Corselli, C., 2009. Shallow seep related seafloor features along the Malta plateau (Sicily channel – Mediterranean Sea): Morphologies and geo-environmental control of their distribution. Marine and Petroleum Geology, 26, 1831-1848.

Savini, A., Pinson, S., Bistacchi, A., Etiope, G., Holland, C., submitted. Imaging shallow migration pathways in a mud volcano province using an autonomous underwater vehicle (Malta Plateau, Mediterranean Sea). Near Surface Geophysics.

Stakes, D.S., Orange, D., Paduan, J.B., Salamy, K.A., Maher, N., 1999. Cold-seeps and authigenic carbonate formation in Monterey Bay, California. Marine Geology 159, 93-109.

Stirling, C.H., Esat, T.M., McCulloch, M.T., Lambeck, K., 1995. High-precision U-series dating if corals from Western Australia and implications for the timing and duration of the Last Interglacial. Earth Planetary Science Letters 135, 115-130.

Tonarelli, B., Turgutcan, F., Max, M.D., Akal T., 1993. Shallow sediments at four localities on the Sicilian–Tunisian Platform, in: Max, M.D., Colantoni, P. (Eds.), UNESCO Technical Reports in Marine Science, Urbino, pp. 123-128.

Tranchida, G., Bellanca, A., Angelone, M., Bonanno, A., Langone, L., Mazzola, S., Neri, R., Patti, B., 2010. Chronological records of metal deposition in sediments from the Strait of Sicily, central Mediterranean: Assessing natural fluxes and anthropogenic alteration. Journal of Marine System 79, 157–172.

Vai, G.B., Cantelli, L., 2004. Litho-palaeoenvironmental maps of Italy during the last two climatic extremes. Map. 1 – Last Glacial Maximum; Map. 2 – Holocene climatic optimum, 1:1.000.000 scale. 32nd I.G.C. Florence.

Waelbroeck, C., Labeyrie, L., Michel, E., Duplessy, J.C., McManus, J.F., Lambeck, K., Balbon, E., Labracherie, M., 2002. Sea-level and deep water temperature changes derived from benthic foraminifera isotopic records. Quaternary Science Review 21, 295-305.

Woelkerling, W.J., 1988. The Coralline Red Algae: an analysis of the genera and subfamilies of non-geniculate Corallinaceae, British Museum Natural History Press.

Yellin-Dror, A., Grasso, M., Ben-Avraham, Z., Tibor, G., 1997. The subsidence history of the northern Hyblean plateau margin, southeastern Sicily. Tectonophysics 282, 277-289.

CAPTIONS

Figure 1 Geographical and geomorphological setting of the studied area: A) Geographical setting: Italy; B) Magnification of Sicily Island with the indication of studied area; C) Digital terrain model of the surveyed area; D) Side Scan Sonar (SSS) photomosaic with the location of sparker profile (black line, transect 1-2); E) magnification of the surface of the tabular relief on SSS mosaic; F) Sparker profile crossing the tabular relief structure. In C, D and E: yellow star indicates the site of core MV03-GC02; black star indicates the site of core MV02-GC01.

Figure 2 Photographs, lithologies, samples and paleoenvironments of the studied cores (see Fig. 1C, 1D for locations). M indicates samples for mollusk identification, B indicates samples collected for U/Th dating. Reliable samples for dating are indicated by the red outline. M15 of core MV02_GC01 and M10 of core MV03-GC02 are the core catchers. M0 of core MV03_GC02 is the top of the core. M9 of core MV03-GC02 is the base of the core.

Figure 3 Biogenic framework from the original cores, before the sample collection. Red point lines highlight the biogenic frameworks.

Figure 4 Sample M12 of core GC01-MV02: A) Details of the level between 132 and 156 cm where sample M12 has been collected. B-D) The three typologies of grains recognized in sample M12: B) Group 1: terrigenous, smooth pebbles partially covered by a thin black coating; C) Group 2: biogenic pebbles rarely covered by a thin black coating, mollusk above the dashed line and fragment of algal concretion below; D) Group 3: biogenic and terrigenous pebbles almost totally covered by a dark smooth coating.

Figure 5 Bioclasts of group 2 including A) *Bittium* sp.; B) *C. rustica*; C) operculum of *Bolma rugosa*; D) Trochidae sp.); E) crustacean fragment: decapod claws; F) echinoid fragment: the base of an echinoid spine; G-H) coated cobbles.

Figure 6 Histograms of the cumulate percentage of mollusks species grouped on the base of their ecological meaning along core MV02-GC01 (A) and MV03-GC02 (B) and related paleodepth reconstruction.

Figure 7 Thin section photographs of M12 sample: A) A fertile specimen of *Titanoderma* sp. with abundant uniporate conceptacles and typical palisade cells; B) *Titanoderma* sp.enveloping a micritic nucleus with badly preserved biogenic particles; *Halimeda* on bottom left; C) A small fragment of *L. stictiforme* showing a blackened contour; D) *L. stictiforme* with abundant uniporate (presumed sporangial) conceptacles; B-D-E) *Halimeda* sp. fragments; F-G-H) Details of the black patina on coralline algae. Scale bar = 100µm.

Figure 8 EDX analyses and SEM images: A) EDX graph of fragment with black coating showing high Ca-sulfate and Al-Mg silicate; B) EDX graph of biogenic fragment with black coating with high carbon peak; C) EDX graph of a fragment of encrusting coralline algae showing high-Mg calcite peak; D) SEM image of a fragment of encrusting coralline algae. Black star indicates the point of EDX analysis showed in C; E) SEM image of the black coating shows a fibrous and very porous nature, with frequent on its surface; F) iron-sulphur framboid spherules on polished thin section, observed also on polished thin sections.

Figure 9 X-ray diffraction results of A-B) a bivalve shell partially encrusted by the black coating and C) a dark lithoclast; D) graph of the shell in A and B that once cut reveals the occurrence of a thin encrustation by dark coralline algae (black arrow); E) X-ray analysis of the lithoclast showed in C.

Figure 10 Paleo sea-level reconstruction at the LGM for the area of the studied tabular relief. Black line indicates the paleo-coast, whereas the light-blue line corresponds to the 10 m isobath. Reconstructed cores location testified the paleo-infralittoral position. The pictures show the succession of deepening upward facies.

Table 1 Table with the list of biocenotic meaningful mollusk species *per* sample of core MV02-GC01. Colors for lines from M0 to M15 indicate: white for silt, light-gray for silty sand, gray for gravelly sand, dark-gray for samples M12. Acronyms follow Pérès and Picard, (1964). AP = *Algues Photophiles* biocoenosis; HP = *Herbier à Posidonie* biocoenosis; SFBC = *Sables fins bien classés* biocoenosis; C = *Coralligène* biocoenosis; DC = *Detritique Côtier* biocoenosis; VTC = *Vase Terrigène Côtier* biocoenosis, VP = *Vase Profonde* biocoenosis; SGCF = *Sables grossiers et des fins Graviers sous l'influence des Courants de Fond* biocoenosis; PE = *Peuplement Hétérogène* biocoenosis.

Table 2 List of the ecologically meaningful mollusk species per sample, core MV03-GC02. Line colors from M0 to M10 indicate: very dark-gray = gravel, white = mud, light-gray = silty sand. For acronyms, referred to caption of Table 1.

Table 1

		Infralittoral zone	Circalittoral zone		Infra- to circalittoral zone
			Coralligenous	**Soft substrate**	
MV02 - GC01	M0			*A. longicallus* (excl VP)	
	M1		*M. perversus* (C)	*A. longicallus* (excl VP) *M. alba* (excl DC) *P. papillosum* (pref DC) *P. rudis* (pref DC) *A. punctura* (DC)	
	M2	*M. attenuata* (excl SFBC) *F. hyalinus* (excl HP) *T. corbuloidea* (excl HP)		*P. jacobaeus* (excl DC) *A. prismatica* (excl DC) *A. tetragona* (pref DC) *P. rudis* (pref DC) *A. punctura* (DC)	
	M3	wood fragment			
	M4	*T. corbuloidea* (excl HP)	*M. pesfelis* (exc C)	*P. jacobaeus* (excl DC) *A. tetragona* (pref DC) *P. rudis* (pref DC) *P. papillosum* (pref DC) *T. communis* (pref VTC) *A. punctura* (DC)	
	M5	*T. corbuloidea* (excl HP) *G. miliaria* (excl HP)	*C. tubercularis* (C)	*P. jacobaeus* (excl DC) *T. turbona* (excl DC) *P. papillosum* (pref DC) *A. tetragona* (pref DC) *P. rudis* (pref DC) *A. punctura* (DC) *E. rosea* (DC/C) *A. nitida* (excl VTC) *T. communis* (pref VTC)	
	M6	*G. miliaria* (excl HP) *A. discors* (HP)	*C. tubercularis* (C) *R. horrida* (C)	*T. turbona* (excl DC) A. tetragona (pref DC) E. rosea (DC/C) *T. communis* (pref VTC)	
	M7	*H. sanguineum* (HP/C) *A. discors* (HP)	*M. perversus* (C) *C. tubercularis* (C) *R. horrida* (C)	*P. jacobeus* (excl DC) *G. fervensis* (excl DC) *T. turbona* (excl DC) *A. tetragona* (pref DC) *P. rudis* (pref DC) *A. punctura* (DC) *T. communis* (pref VTC)	
	M8	*T. corbuloidea* (excl HP)	*C. tubercularis* (C) *R. horrida* (C)	*L. subauriculata* (excl DC) *T. turbona* (excl DC) *A. punctura* (DC) *E. rosea* (DC/C) *A. longicallus* (excl VP)	*D. lupinus* (excl PE)
	M9	*R. bruguieri* (excl HP) *A. discors* (HP) *C. rustica* (excl AP) *R. lilacina* (AP) *H. sanguineum* (HP/C)	*C. tubercularis* (C) *R. horrida* (C)	*T. turbona* (excl DC) *A. tetragona* (pref DC) *A. punctura* (DC)	*G. glycymeris* (excl SGCF)
	M10	*H. sanguineum* (HP/C)	*C. tubercularis* (C)	*T. turbona* (excl DC) *G. fervensis* (excl DC) *A. tetragona* (pref DC)	
	M11/1	*C. rustica* (excl AP) *R. lilacina* (AP) *A. discors* (HP)	*R. echinata* (pref C) *C. tubercularis* (C) *R. horrida* (C)	*A. tetragona* (pref DC) *A. punctura* (DC)	
	M11/2	*R. lilacina* (AP) *H. sanguineum* (HP/C)	*R. horrida* (C)	*P. rudis* (pref DC)	
	M11/3	*R. lilacina* (AP) *R. bruguieri* (excl HP) *G. miliaria (excl HP)* *G. ardens* (HP) *A. discors* (HP) *H. sanguineum* (HP/C)	*M. perversus* (C) *C. tubercularis* (C)	*A. punctura* (DC)	

	M12	*V. verrucosa* (exp HP) *R. bruguieri* (excl HP) *G. miliaria* (excl HP) *G. albida* (HP) *A. discors* (HP) *C. rustica* (excl AP) *R. lilacina* (AP) *H. sanguineum* (HP/C)	*C. tubercularis* (C) *M. perversus* (C) *R. horrida* (C)	*T. communis* (pref VTC) *A. punctura* (DC)	
	M13	*R. auriscalpium* (AP) *R. lilacina* (AP) *A. discors* (HP) *H. sanguineum* (HP/C)	*M. perversus* (C) *C. tubercularis* (C)	*T. turbona* (excl DC) *A. tetragona* (pref DC) *M. cristata* (pref DC) *T. communis* (pref VTC)	*G. glycymeris* (excl SGCF) *T. villosiuscula* (excl SGCF)
	M14	*R. lilacina* (AP)	*C. tubercularis* (C) *R. horrida* (C)		
	M15	*R. lilacina* (AP)	*C. tubercularis* (C)		

Table 2

		Infralittoral zone	Circalittoral zone		Infra- to circalittoral zone
			Coralligenous	Soft substrate	
MV03 - GC02	M0	*F. fabula* (excl SFBC)	P. incomparabile (excl C)	*T. turbona* (excl DC) *A. tetragona* (pref DC)	*D. lupinus* (excl PE)
	M1	*T. corbuloidea* (excl HP)	*P. incomparabile* (excl C) *M. pesfelis* (C) *M. perversus* (C)	*A. tetragona* (pref DC) *P. papillosum* (pref DC) *P. rudis* (pref DC)	*T. villosioscula* (excl SGCF) *G. glycymeris* (SGCF) *D. lupinus* (excl PE)
	M2	*T. corbuloidea* (excl HP)		*A. longicallus* (excl VP) *A. tetragona* (pref DC) *P. rudis* (pref DC) *G. minima* (DC)	
	M3	*C. rustica* (excl AP) *N. josephinia* (ecl SFBC)	*P. incomparabile* (excl C) *M. pesfelis* (C)	*A. tetragona* (pref DC) *P. papillosum* (pref DC) *P. rudis* (pref DC) *G. minima* (DC) *E. rosea* (DC/C)	
	M4	*A. discors* (HP) *H. sanguineum* (HP/C)		*A. longicallus* (excl VP) *T. turbona* (excl DC) *A. tetragona* (pref DC) *P. rudis* (pref DC)	*G. glycymeris* (SGCF)
	M5	*R. bruguieri* (excl HP) *A. discors* (HP) *N. josephinia* (excl SFBC) *H. sanguineum* (HP/C)	*M. pesfelis* (excl C) *M. perversus* (C) *C. tubercularis* (C)	*T. turbona* (excl DC) *P. papillosum* (pref DC)	
	M6	*N. josephinia* (excl SFBC) *A. discors* (HP) *R. lilacina* (AP) H. *sanguineum* (HP/C)	*R. echinata* (pref C) *M. perversus* (C) *C. tubersularis* (C)	*T. turbona* (excl DC) *P. papillosum* (pref DC) *A. punctura* (DC)	
	M7	*R. bruguieri* (excl HP) *A. discors* (HP) *R. lilacina* (AP) *H. sanguineum* (HP/C)	*M. perversus* (C) *C. tubercularis* (C)	*T. turbona* (excl DC) *A. tetragona* (pref DC)	
	M8	R. lilacina (AP) *H. sanguineum* (HP/C)	*C. tubercularis* (C)	*A. punctura* (DC)	
	M9	*R. lilacina* (AP) *A. discors* (HP)	*M. perversus* (C) *C. tubercularis* (C)	*T. turbona* (excl DC) *A. punctura* (DC)	
	M10	*C. rustica* (excl AP) R. lilacina (AP) R. bruguieri (excl HP) *A. discors* (HP) *N. josephinia* (excl SFBC)	*M. perversus* (C) *C. tubercularis* (C) *R. horrida* (C)	*T. turbona* (excl DC) *A. punctura* (DC)	

Highlights

Two cores have been collected in a tabular relief at 140 m wd south of Sicily

Paleoecology analyses reveal sediments related to diverse climatic phases

Bioconstruction shows features comparable to present day algal reef (coralligenous)

Coralligenous unveils a poliphasic origin of both warm and glacial stages

Last low stand deposits are really peculiar with dark patina and recrystallization

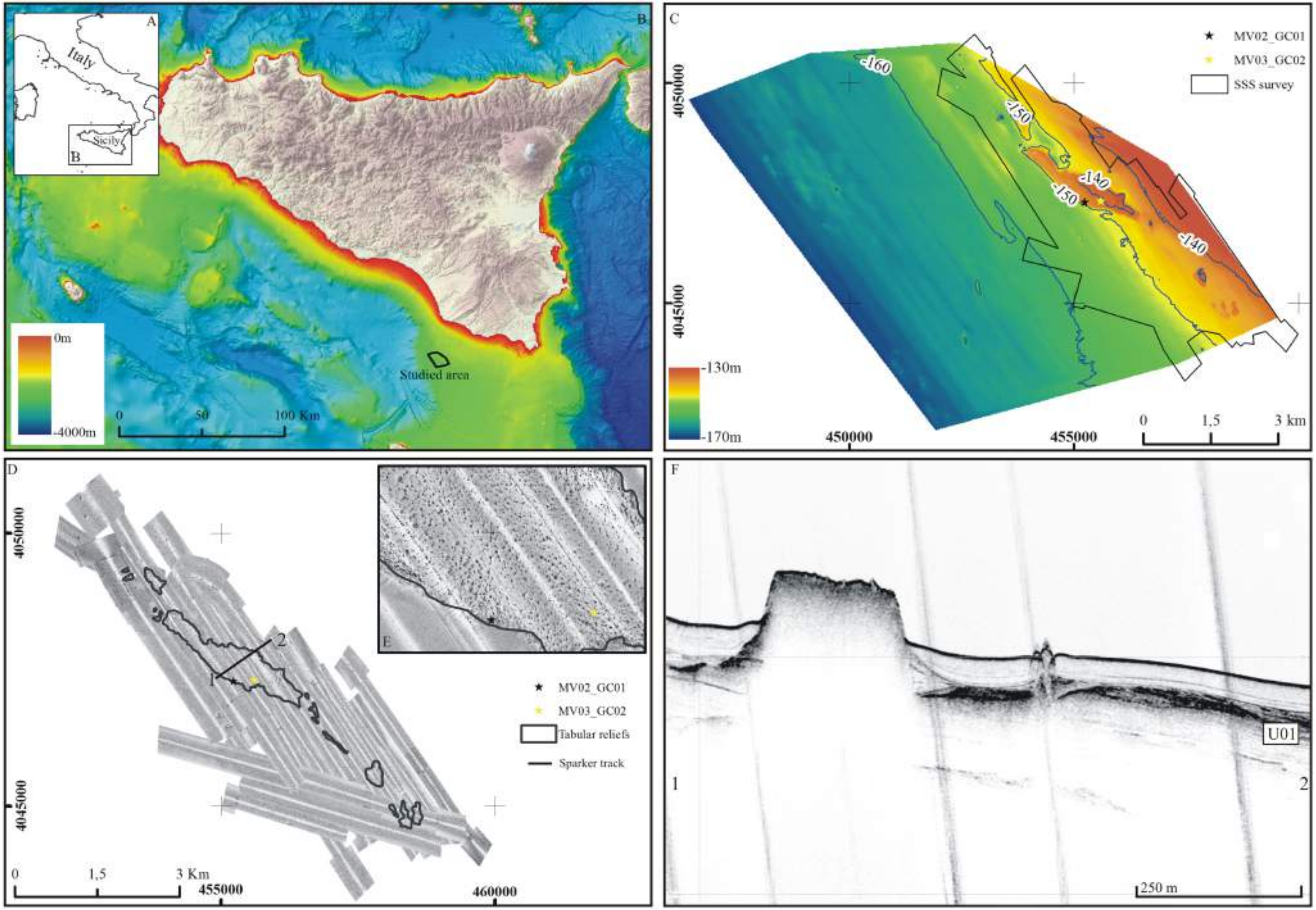
A
Italy
Sicily
B
0m
-4000m
Studied area
0
50
100 Km
C
MV02_GC01
MV03_GC02
SSS survey
-160
-150
-140
-150
-140
4050000
4045000
-130m
-170m
450000
455000
0
1,5
3 km
D
4050000
4045000
2
1
E
MV02_GC01
MV03_GC02
Tabular reliefs
Sparker track
0
1,5
3 Km
455000
460000
F
U01
1
2
250 m

Figure 1

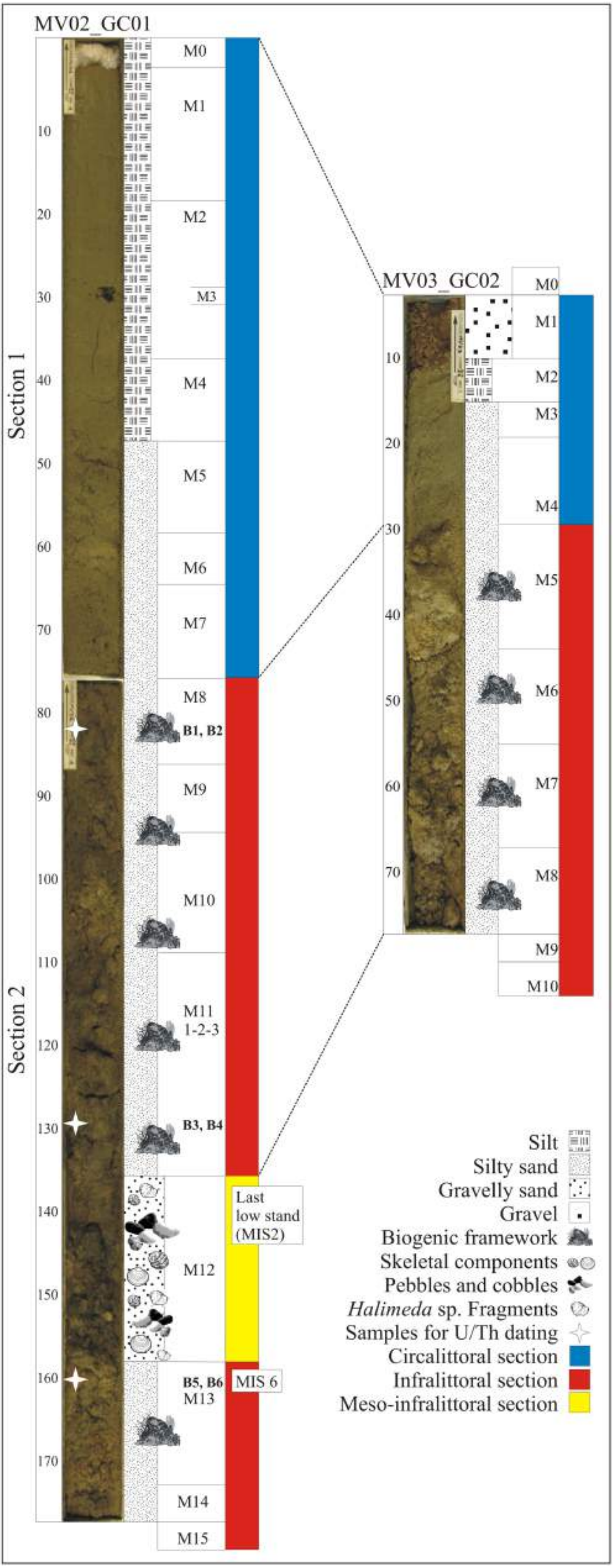
MV02_GC01
Section 1
Section 2
10
20
30
40
50
60
70
80
90
100
110
120
130
140
150
160
170
M0
M1
M2
M3
M4
M5
M6
M7
M8
B1, B2
M9
M10
M11
1-2-3
B3, B4
M12
B5, B6
M13
M14
M15
Last
low stand
(MIS2)
MIS 6
MV03_GC02
M0
M1
M2
M3
M4
M5
M6
M7
M8
M9
M10
Silt
Silty sand
Gravelly sand
Gravel
Biogenic framework
Skeletal components
Pebbles and cobbles
Halimeda sp. Fragments
Samples for U/Th dating
Circalittoral section
Infralittoral section
Meso-infralittoral section

Figure 2

Figure 3

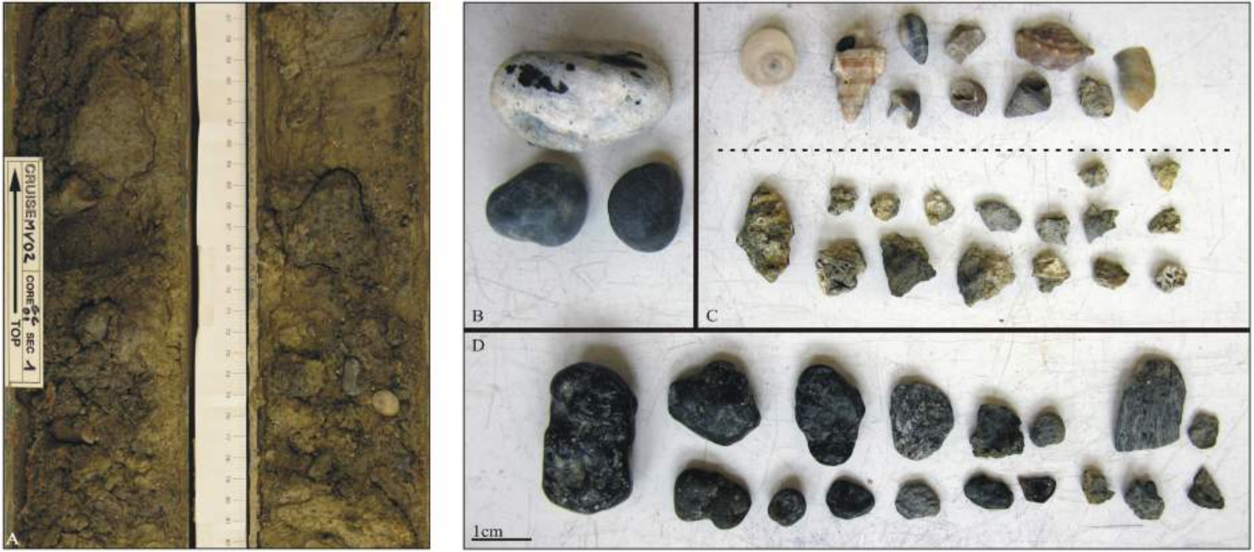

Figure 4

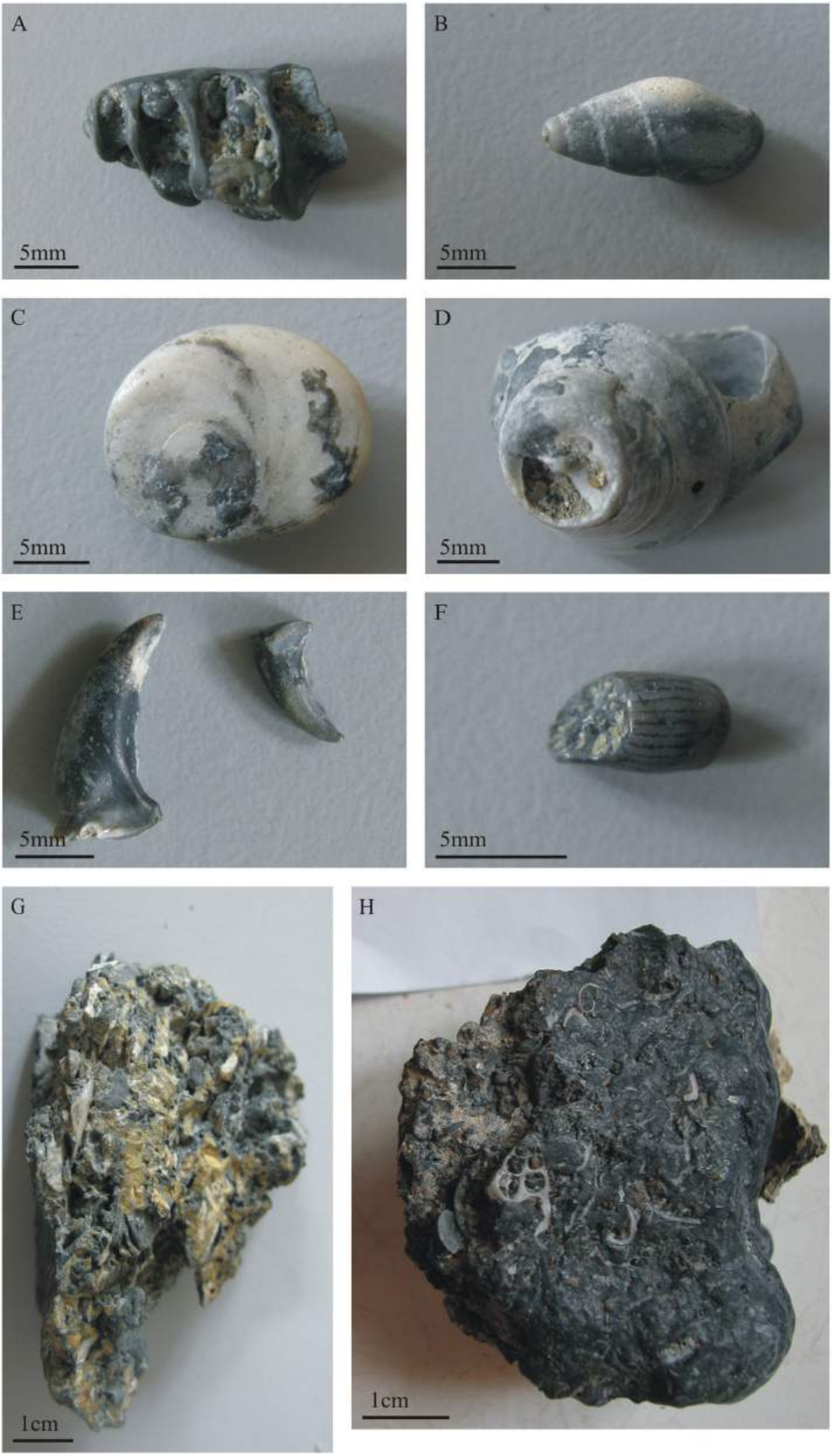

Figure 5

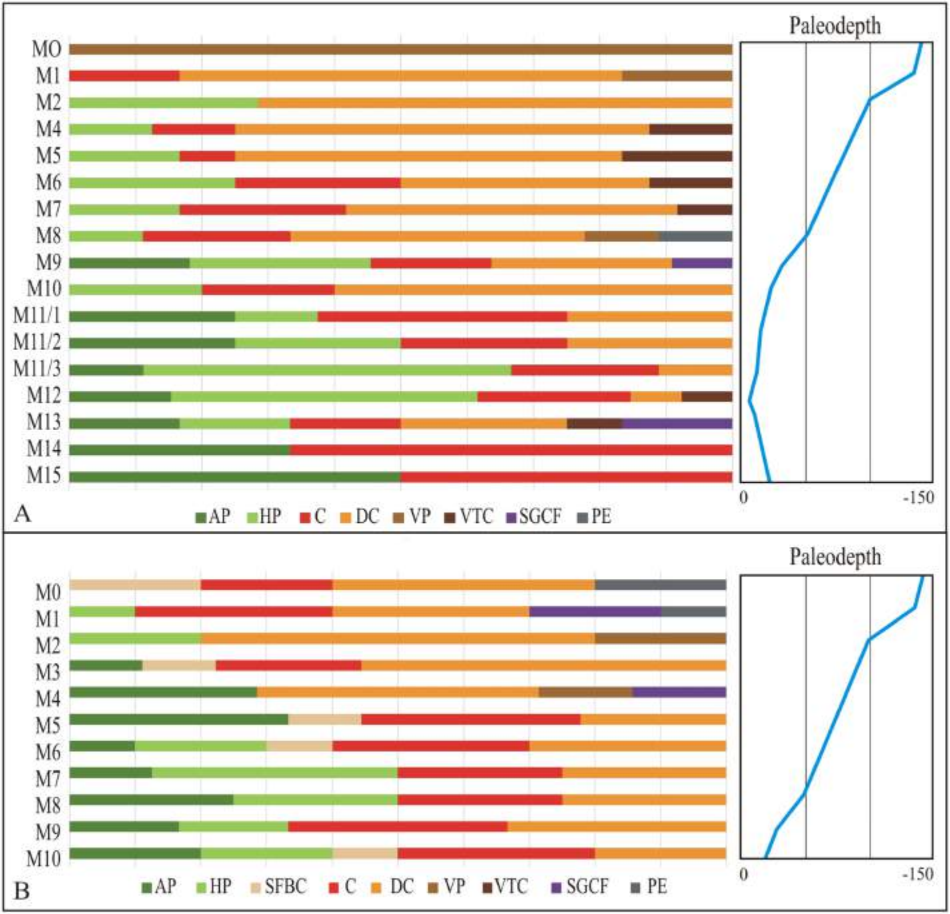
Paleodepth
M0
M1
M2
M4
M5
M6
M7
M8
M9
M10
M11/1
M11/2
M11/3
M12
M13
M14
M15
0
-150
A
AP
HP
C
DC
VP
VTC
SGCF
PE
Paleodepth
M0
M1
M2
M3
M4
M5
M6
M7
M8
M9
M10
0
-150
B
AP
HP
SFBC
C
DC
VP
VTC
SGCF
PE

Figure 6

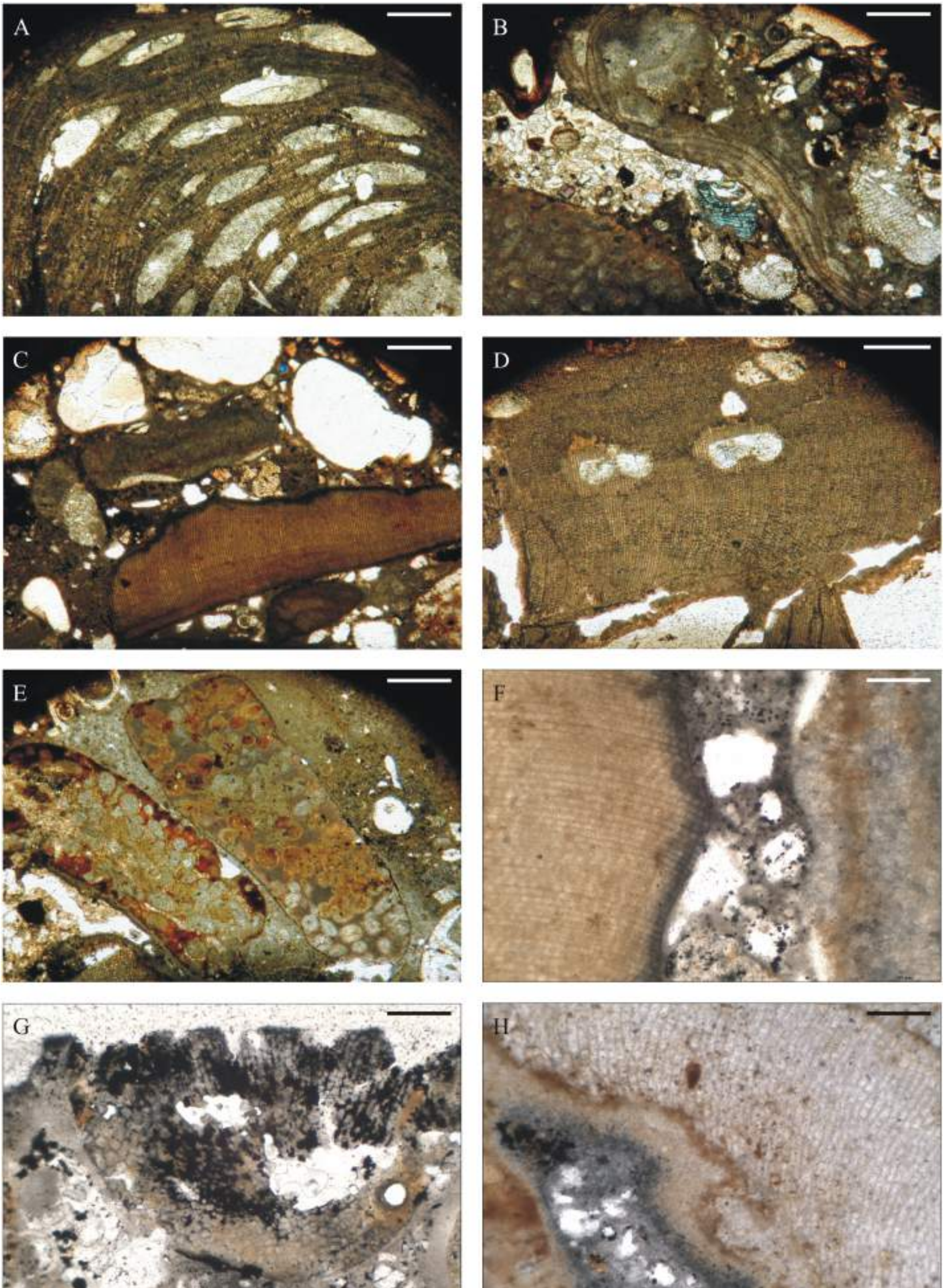

Figure 7

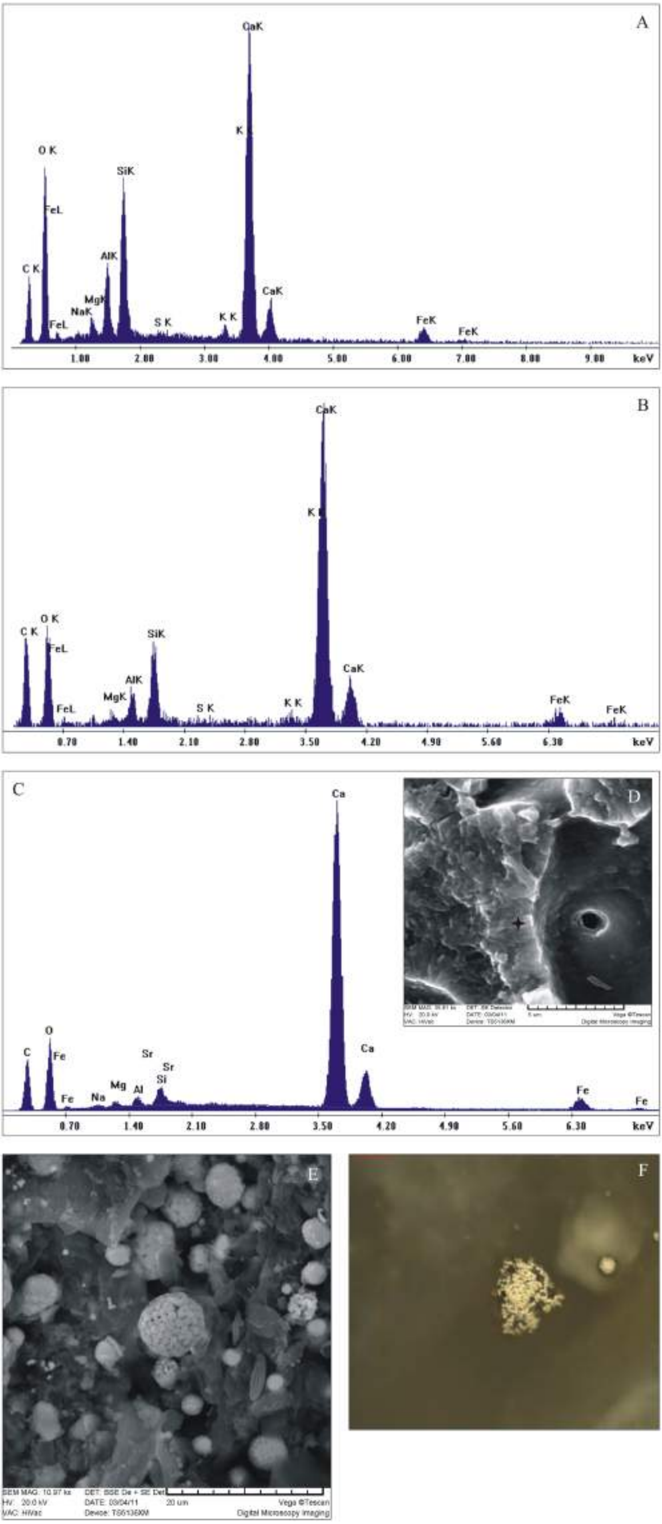
A
CaK
K
O K
SiK
FeL
AlK
C K
MgK
NaK
FeL
S K
K K
CaK
FeK
FeK
1.00
2.00
3.00
4.00
5.00
6.00
7.00
8.00
9.00
keV
B
CaK
K K
O K
C K
FeL
SiK
AlK
MgK
FeL
S K
K K
CaK
FeK
FeK
0.70
1.40
2.10
2.80
3.50
4.20
4.90
5.60
6.30
keV
C
Ca
O
C
Fe
Sr
Sr
Si
Mg
Al
Na
Fe
Ca
Fe
Fe
0.70
1.40
2.10
2.80
3.50
4.20
4.90
5.60
6.30
keV
D
E
SEM MAG: 10.97 kx
DET: BSE De + SE Det
HV: 20.0 kV
DATE: 03/04/11
20 um
Vega ©Tescan
VAC: HiVac
Device: TS5136XM
Digital Microscopy Imaging
F

Figure 8

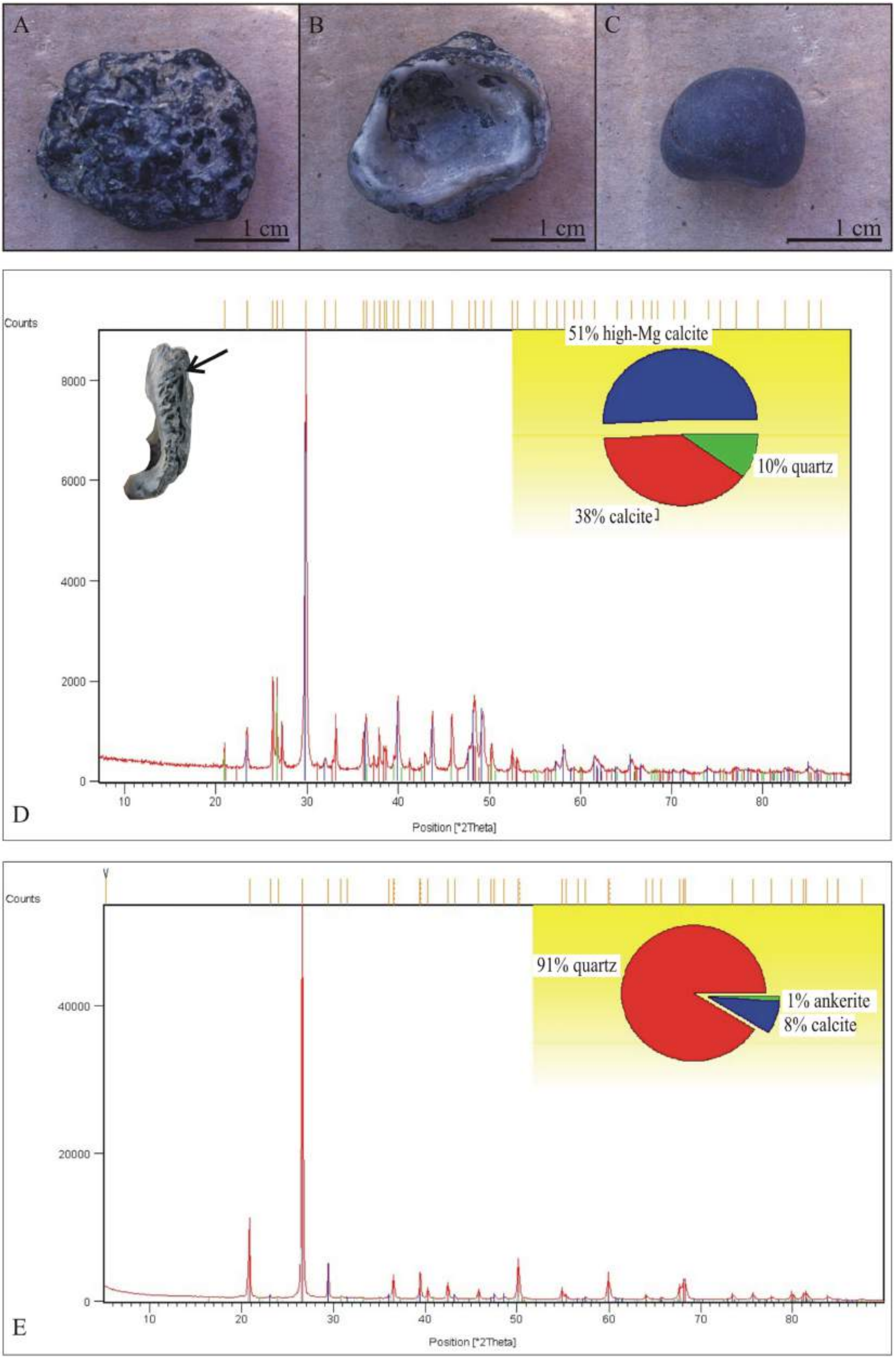
A
1 cm
B
1 cm
C
1 cm
Counts
51% high-Mg calcite
10% quartz
38% calcite
8000
6000
4000
2000
0
10
20
30
40
50
60
70
80
D
Position [°2Theta]
Counts
91% quartz
1% ankerite
8% calcite
40000
20000
0
10
20
30
40
50
60
70
80
E
Position [°2Theta]

Figure 9

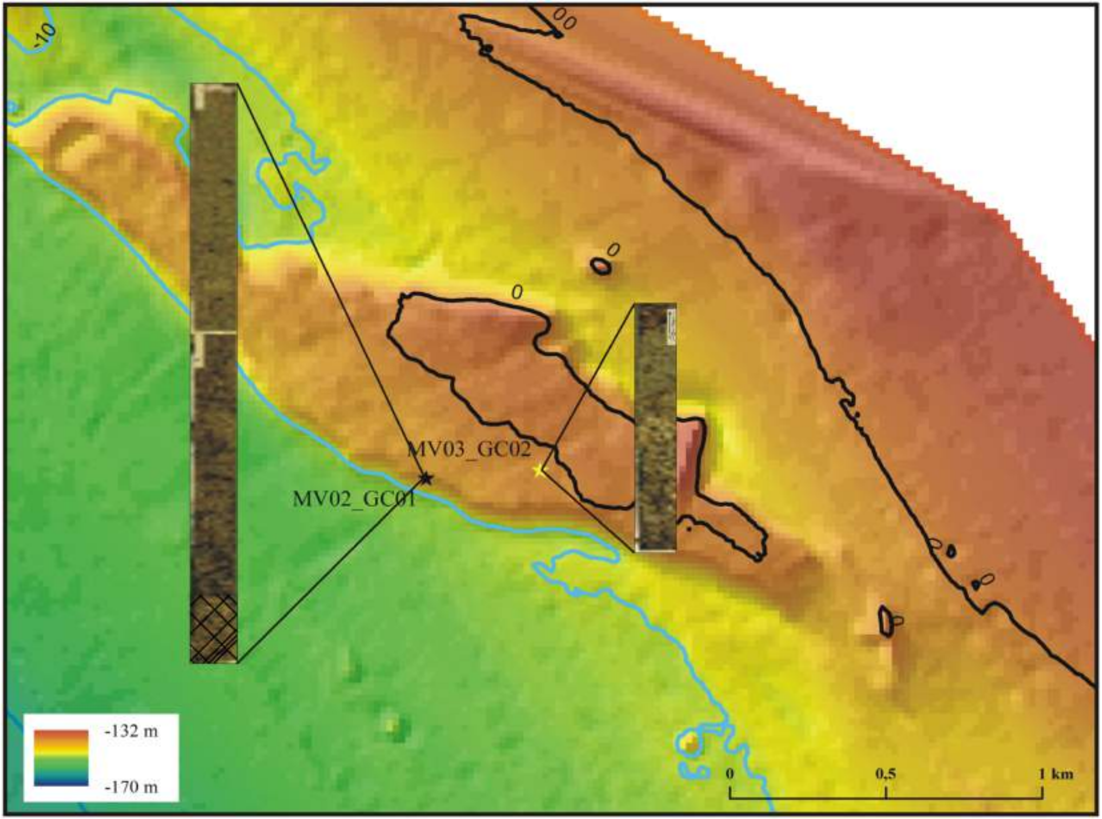

Figure 10